Hindawi
Advances in Civil Engineering
Volume 2024, Article ID 2994221, 10 pages
https://doi.org/10.1155/2024/2994221

Research Article

Thermal Performance Assessment of Concrete Walls Using Different Phase Change Materials

Muhammad Usman,[1] **Mahmood Hussain**,[1] **Arslan Mushtaq**,[1] **Syed H. Farooq**,[1] **Atif Mehmood**,[1] **and Asad Hanif**[2,3]

[1]*School of Civil and Environmental Engineering, National University of Sciences and Technology, Sector H-12, Islamabad, Pakistan*
[2]*Civil and Environmental Engineering Department, King Fahd University of Petroleum and Minerals (KFUPM), Dhahran 31261, Saudi Arabia*
[3]*Interdisciplinary Research Center for Construction and Building Materials, King Fahd University of Petroleum and Minerals (KFUPM), Dhahran 31261, Saudi Arabia*

Correspondence should be addressed to Asad Hanif; ahanif@connect.ust.hk

Received 24 October 2022; Revised 16 March 2024; Accepted 18 March 2024; Published 14 May 2024

Academic Editor: Esra Mete Güneyisi

Energy demand is continuously increasing around the globe, and the building sector contributes 40% of the total energy consumption, as per the studies. Fossil fuels are the primary cause of harmful gas emissions, thus causing environmental pollution. There is a dire need to introduce innovative techniques to fulfill energy demands while reducing environmental pollution. Phase change materials (PCMs) are the latent thermal storage materials that store thermal energy during phase change from solid to liquid state and vice versa. Thus, using PCMs in structural engineering offers one of the best options for rapidly developing energy-saving materials. To do so, ascaled model, concrete walls room, encapsulating locally available PCMs, was constructed in this study. Three locally available PCMs (glycerin, vegetable ghee, and ferric chloride hexahydrate) have been tested in a controlled environment. The model response is then evaluated for the energy-storing capacity of each PCM while considering the human comfort zone. From the test results, it is concluded that PCMs have a significant effect on improving the thermal energy efficiency of the model without any notable adverse effects. Over the completion of the test, after 12 hr, all the incorporated PCM showed positive results, and a maximum temperature loss of 2.25 K was observed. Among different PCMs, the optimal performance was observed for vegetable ghee, which showed a drop in temperature for all the points at the inner side of the wall, i.e., $T3$, $T4$, and $T5$.

1. Introduction

Energy demand is a critical issue that needs to be addressed as energy consumption is increasing day by day due to exponential growth in the population. As per the energy technology perspectives (ETP) report, the building sector accounts for 34% of global energy demand. In order to meet the energy requirement, fossil fuels are burnt to produce electricity in thermal power plants, which affects the environment and causes the depletion of natural resources. However, many efforts are being made to switch from nonrenewable to renewable energy resources, i.e., wind energy and solar energy. Apart from replacing energy production methods, efforts are being made to conserve the energy where it is being utilized. One such step is modifying the intrinsic properties of the concrete, which is used to make the buildings where energy is utilized.

Consequently, researchers from the construction industry are paying more attention to developing energy-saving materials known as green building materials [1, 2]. To deal with critical energy situations and save a portion of energy in the buildings, enhancing the energy storage capacity of concrete is imperative. For massive concrete construction, innovative materials such as their intrinsic thermal properties can be effective for concrete, i.e., to store thermal energy during the day and release it slowly at night [3]. Introducing phase change material (PCM) in concrete mixes can be quoted as a suitable example in such cases [4–6]. PCM materials can be defined as "Phase change, are the latent heat of storage, materials can store a large amount of thermal energy in its phase change from solid to liquid or vice versa." Generally, thermal energy storage materials are of two types:

(i) Sensible heat storing.
(ii) Latent heat storing.

PCM has become necessary with the increase in energy demands. Buildings have been the primary energy consumers and require necessary modifications in architectural and material aspects. A limited number of studies have been carried out previously to incorporate PCMs. Small-scale indoor tests were conducted using the PCMs in lightweight aggregate (LWA) to measure their performance in residential buildings. It was concluded that the macroencapsulation of paraffin LWA reduced the internal surface temperature by 4.7–7.5 Kelvins (K), with a further reduction of 2.9 K in the internal room temperature [3]. Another investigation of the thermal performance of PCMs was conducted using the full-scale model and employing numerical analysis techniques. In this investigation, two PCM panels containing capric acid (PCMOW) and 1-dodecanol (PCMIW) were installed on the outside and inside surfaces of the walls and roofs. It was concluded that PCMIW showed a better performance [7].

Besides the macroencapsulation techniques, other techniques have been used to incorporate PCM in the wall. Trombe walls have been used and found efficient in reducing internal temperatures. These walls were made using salt hydrates and hydrocarbons as PCMs [8]. Sharma et al. [9] have researched two passive storage collector walls using calcium chloride hexahydrate (melting point 571.15 K) as a PCM. It was concluded that an 8.1 cm PCM wall has slightly better thermal performance than a 40 cm thick masonry wall [9]. A new technique of incorporating the PCM at the microscopic level is also in vogue these days [10]. PCM-based window shutters are also being used to achieve better internal temperature. In this case, a movable shutter made of PCM is placed inside the window. During the daytime, the shutter is opened to expose the shutter to direct sunlight to absorb the heat. Later on, the PCM shutter is closed at night, and the absorbed heat from the PCM radiates into the room. A temperature drop of 2 K has been reported [9]. Zalewski et al. [8] established a composite solar wall to store a large amount of heat energy in a small volume, making it possible to use as a lightweight arrangement. The composite solar wall consists of several layers: a semitransparent cover, a closed cavity, a storage wall, a ventilated air cavity, and insulating panels where two vents allow the warm air to enter the room. PCM bricks are incorporated into the solar wall to store heat energy [8]. Shi et al. [11] conducted an experimental study to assess the effect of change in installation positions of macroencapsulated PCM in concrete walls on indoor temperatures and humidity levels. The results indicated that the model with PCM laminated within the concrete walls showed better temperature control and effectively reduced the maximum temperature by up to 4 K. However, the model with PCM placed on the inner side of concrete walls showed the best humidity control and reduced the relative humidity by 16% more than the control model [11].

Table 1: Chemical composition of cement.

Oxides	Wt. (%)
SiO_2	20
Al_2O_3	6.04
Fe_2O_3	4.24
CaO	60.7
MgO	2.06
SO_3	2.01
LOI	1.83

Different researchers have researched methods for measuring the thermophysical properties and the classification of PCMs based on applications and temperature ranges [12–14]. Due to excellent thermal and physical characteristics, organic PCMs have great potential, especially in low- to medium-temperature-TES applications [15]. This confirms that one of the important, potential, and advanced applications of PCMs is building heating management, i.e., heating and cooling [12, 16]. Nevertheless, critical attention has been given to PCM composites and PCM-based photovoltaic thermal systems, which have emerged as promising materials for building use [17, 18]. There are many studies on incorporating PCM in cement mortars as cement composites [19–22]. Cunha et al. [22] developed four innovative mortars directly incorporating PCMs and determined the PCM influence on the resulting physical, mechanical, and thermal properties. It was confirmed that the physical and mechanical behaviors were significantly changed. Also, 20% incorporation of PCM was found optimal. Similar findings were reported by Rebelo et al. [21] for mortars incorporated with two different microencapsulated PCMs. The beneficial effects of PCMs were also experimentally assessed for TES mortars, and the results were numerically validated [19, 20].

There are many studies done on the composites of PCM, but less work has been done on isolated PCM-based configuration as a TES material. This research aims at the utility of three different PCMs, ferric chloride, glycerin, and vegetable ghee (locally available as DALDA), in concrete to check and compare their feasibility as a suitable thermal energy storage material in buildings. This investigation has been carried out to identify the best thermal storage material among the three PCMs used in the model.

2. Experimental Program

In the first phase, all the material used and the casting process are discussed concisely, while the second phase covers the cyclic thermal loading that was carried out to make the observations.

2.1. Materials and Methods

2.1.1. Cement. Portland cement with an average particle size of 15.41 microns, conforming to ASTM C150, was used. Table 1 shows the chemical composition of Bestway cement.

2.1.2. Fine and Coarse Aggregate. Fine aggregate was obtained from Lawrencepur source. Sand used is coarse sand, having a

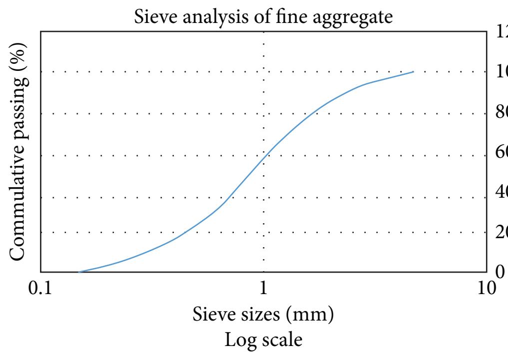

Figure 1: Gradation curve of fine aggregate.

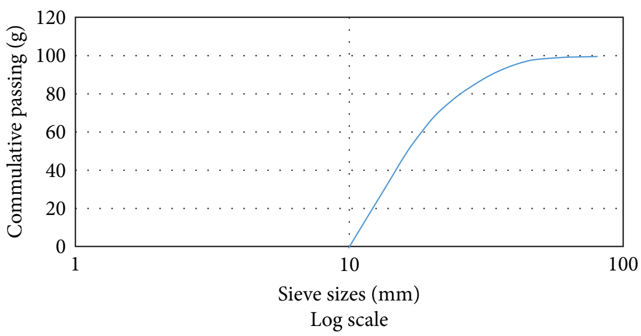

Figure 2: Gradation curve of coarse aggregate.

Table 2: Aggregate properties.

Coarse aggregate absorption	0.98%
Fine aggregate absorption	2.4%
Fineness modulus of sand	3.46

fineness modulus of 3.46. The specific gravity of sand was calculated as 3.42. Coarse aggregate was procured from Margalla Hills quarry, Islamabad. Both the aggregate, coarse and fine have been graded as per ASTM gradation envelope, as shown in Figures 1 and 2. The physical properties of coarse aggregate are shown in Table 2.

2.1.3. Phase Change Material. While conducting this study, the utmost effort was made to bring those materials to the experimentation, which is locally available and economical. In this regard, three choices were made as follows:

(a) Ferric chloride hexahydrate ($FeCl_3{\cdot}6H_2O$).
(b) Glycerin.
(c) Vegetable ghee.

In the literature, ferric chloride hexahydrate and glycerin have been reported as phase-change materials. However, during the identification for PCM, the locally used vegetable ghee shows some tendencies for being used as PCM. Therefore, it was decided that the third PCM for this study shall be vegetable ghee. The easy availability of vegetable ghee from a local vendor, "Dalda," and the gap in its use as a PCM led to its behavior as a thermal energy storage material in concrete. The ambient temperature and humidity conditions favor the use of vegetable ghee in its in situ state. In order to compare the results and form a fair comparison on the same model, ferric chloride hexahydrate and glycerin were used as the two other PCMs.

(1) Ferric Chloride Hexahydrate ($FeCl_3{\cdot}6H_2O$). Ferric chloride hexahydrate comes with a chemical formula of $FeCl_3{\cdot}6H_2O$. It is available in pale yellow lumps. It has a melting point of almost 310 K and a boiling point of 555.65 K. The latent heat of fusion is about 223 J/kg K. Ferric chloride comes with different trade names. In this study, ferric chloride of "DUKSAN" was used (Figure 3(a)).

(2) Glycerin. Glycerin comes with a chemical formula of $CH_2(OH)CH(OH)CH_2OH$. It is available in a thick, viscous liquid. It has a melting point of almost 292.15 K and a boiling point of 563.15 K. The latent heat of fusion is about 198 J/kg K. Figure 3(b) shows the glycerin used in this study.

(3) Vegetable Ghee. Vegetable ghee comes with a chemical formula of ($C_{17}H_{33}COO$). It is available in a thick, viscous liquid. It has a melting point of almost 303.15 K and a boiling point of 473.15 K. The latent heat capacity of vegetable ghee ranges from 1.67 to 2.5 kJ/kg K. Vegetable ghee is available under different trade names in the market. In this study, vegetable ghee with the trade name "DALDA" has been used, as shown in Figure 3(c).

2.2. Experimental Model. A scaled cubical room of internal dimensions 2′ × 2′ was constructed with the top open. Plain concrete was selected as the material for constructing its walls, having a wall thickness of 6″. The mix ratio used for constructing this model room was 1 : 2 : 4 (one part ordinary Portland cement, two parts well-graded sand, and four parts well-graded coarse aggregates) with 28 days of cylindrical compressive strength of 3,000 psi (Table 3). The water-to-cement ratio was kept at 0.45. The purpose of selecting this mix ratio was to represent the typical concrete used in routine construction in Pakistan.

The model was wet-cured for 7 days and then kept for air curing in a humid atmosphere for another 14 days to achieve the desired compressive strength of concrete. Figure 4 shows a schematic plan of the testing arrangement.

The formwork employed for constructing the model was made of locally available plywood sheets (Figure 5(a)). The steel tubes were used for the encapsulation of the PCM (Figure 5(b)). These tubes were embedded in the face wall of the model with a frontal cover of 1″. The diameter of each tube was 0.7″ with a center-to-center spacing of 2″. The embedded length of each steel tube was 2′. These tubes were covered by steel caps and sealed using RTV silicon rubber sealant.

A temperature data logger was devised locally so as to collect all the data. For this purpose, Arduino Uno, along with DS18B20 thermometers, was used (Figure 5(c)). Each thermometer had a temperature measuring range of 253.15–393.15 K. The Arduino was programed to get the data from these thermometers. The acquired data was converted and saved into an Excel file using MATLAB code. The temperature data acquired were stored against each time date

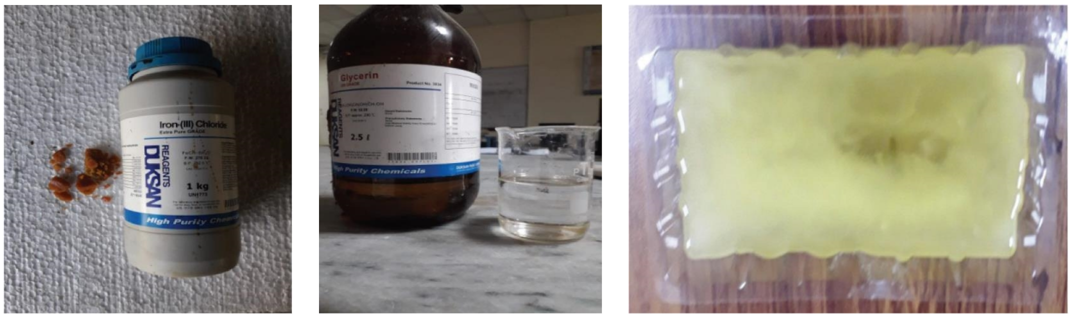

(a) (b) (c)

Figure 3: PCMs used in this study: (a) DUKSAN, (b) glycerin, and (c) vegetable ghee.

Table 3: Mix design of concrete wall.

	Mix design			
Description	Cement (kg/m^3)	Fine aggregate (kg/m^3)	Coarse aggregate (kg/m^3)	Water (kg/m^3)
Concrete (3,000 psi)	316.2	704	1,276	142.2

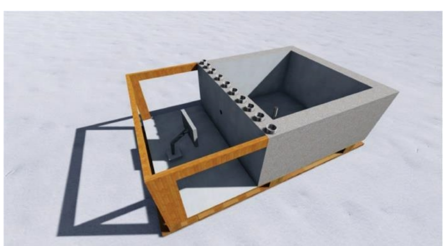

Figure 4: Schematic diagram showing the testing arrangement.

for the entire testing process. The time interval for taking each measurement was 10.2 s.

The heat source used for this study was a 1,000-W fluorescent lamp (Figure 5(d)). The lamp was mounted onto an aluminum-coated cylinder to achieve a height of 1′. The heating arrangement was made in such a way that it focuses on the center of the subject model.

Since the frontal wall of the model was filled with the PCM, the front wall was covered from all four sides except the front. This covering was done using plywood sheets with an inner lining of aluminum foil to optimize the efficiency of the heating source (Figure 6). Any other space was filled with a thermocolsheet. The top open surface of the model was also insulated using the thermocolsheet.

2.3. Testing

2.3.1. Fresh and Hardened Properties of Concrete.

(1) Workability Using Slump Test. The workability of fresh concrete mix has been assessed by the slump test as per ASTM C-143 [23]. Using a scoop, the slump cone was filled in three equal layers by volume prior to pouring in the formwork of the wall incorporating PCMs tubes. Each layer was tamped 25 times with a tamping rod. A drop in the level of fresh concrete after removing the cone was noted and reported as the slump value.

(2) Compressive Strength Using Rebound Hammer. In this research, a rebound hammer was used, which is an indirect method of determining concrete compressive strength as per ASTM C 805-97 [24]. The test was performed on the vertical face of the wall, followed by noting down the rebound number for every point on the wall lying in the mesh of 12 inches by 12 inches, as shown in Figure 7.

(3) Portable Ultrasonic Nondestructive Indicating Test (PUNDIT). To ensure that the difference in temperature is due to the nature of the PCM used, it is essential to make sure that there is no honeycombing in the concrete matrix. To check the homogeneity of the concrete matrix in the hardened state, a portable ultrasonic nondestructive indicating test was performed on the walls of the concrete chamber on which temperature sensors were later installed. The test setup included transmission and receiving transducers that send and receive a timed pulse of ultrasonic energy through the concrete sample. Each face was tested as per ASTM C 597-02 [25] through direct measurement of travel time (in microseconds) for a distance of 300 mm face to face, which is the thickness of the wall of the chamber. Velocity was measured using Equation (1):

$$v = \frac{d}{t}, \tag{1}$$

where v is the velocity mm/μs, d is the distance between sending and receiving transducer, and t is the time taken by signal to travel from one face to the other face

2.3.2. Thermal Performance Testing.

After preparing the experimental model for the testing phase, thermal loading cycles were

Figure 5: PCMs: (a) plywood formwork, (b) PCM steel tubes with caps, (c) thermometers with a data logger, and (d) 1,000 W light.

Figure 6: Heat insulation arrangement.

applied to the samples using a 1,000 W high-intensity lamp, as elaborated above in the following sequence.

(a) The concrete model without any addition of PCM.
(b) The concrete model with front wall tubes filled with glycerin.
(c) The concrete model with front wall tubes filled with vegetable ghee.
(d) The concrete model with front wall tubes filled with ferric chloride hexahydrate.

From thermal loading cycles, the authors mean that the experimental model was continuously subjected to heat energy for some duration and then allowed to cool in ambient atmospheric conditions. The concept behind heating and cooling testing cycles is related to exposure to actual structures, such as high temperatures outside in the daytime and lower temperatures at night. Each PCM of three types was tested separately for heating and cooling cycles.

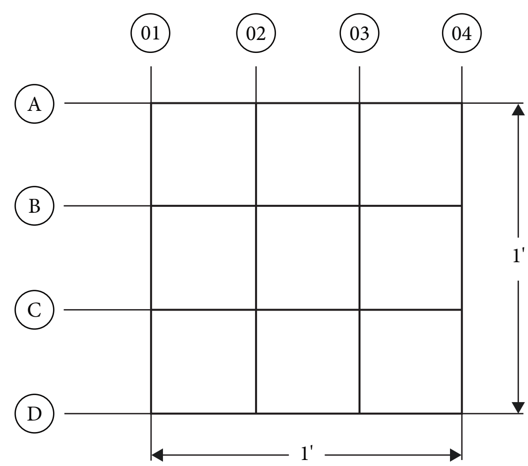

Figure 7: Mesh for rebound hammer.

(i) Three-hour cycle—Three hours of heating followed by 3 hr of cooling in ambient atmospheric conditions. This cycle was repeated twice, with the time required to complete one cycle in 6 hr and the time to complete the test for one type of PCM in 12 hr.
(ii) Two-hour cycle—Two hours of heating followed by 4 hr of cooling in ambient atmospheric conditions. This cycle was repeated twice, with the time required to complete one cycle in 6 hr and the time to complete the test for one type of PCM in 12 hr.

Table 4: Rebound hammer data at 16 points on the face of the wall chamber.

S. no.	Direction of hammer	Rebound point	Rebound number	Average rebound number	Compressive strength (MPa)	Compressive strength (psi)
1	A	A1	28	29	21	3,045
2		A2	28			
3		A3	29			
4		A4	28			
5		B1	26			
6		B2	28			
7		B3	29			
8		B4	28			
9		C1	30			
10		C2	31			
11		C3	31			
12		C4	30			
13		D1	31			
14		D2	32			
15		D3	28			
16		D4	34			

According to ASTM C 805-18: rebound number = 29 rebound number (average).

In each heating session, the model was heated using a 1,000 W halogen lamp placed inside the insulation at the position and location motioned in the previous section. The model without tubes was tested under the same conditions and was selected as the baseline for comparing the performance of PCM.

The temperature was noted at the point with the temperature data logger described in the previous sections. The temperature was recorded at an interval of 10.2 s. All the recorded values were plotted using MATLAB in a time vs. temperature graph.

The temperature for the model at each testing cycle for each PCM (including the base model without PCM) was noted at five locations. The temperature sensors/thermometers were named $T1$, $T2$, $T3$, $T4$, and $T5$, with $T1$ and $T2$ meant to measure the external surface temperature of the concrete wall, whereas $T3$ and $T4$ measured the temperature values on the internal surface of the concrete wall, encasing PCM tubes of the model. The fifth temperature sensor, $T5$, measured the air temperature inside the model.

3. Results

3.1. Fresh and Hardened Properties of Concrete

3.1.1. Workability. The workability of fresh concrete was assessed through a slump test. An average slump value of 85 mm was observed for the mix, having a water-to-cement ratio of 0.45. This shows that the concrete mix had a medium-range workability lying in the range of 50–100 mm for normal concrete as per ACI-301.

3.1.2. Compressive Strength. The compressive strength of the one face of the wall was assessed using Rebound Hammer, and the corresponding results are given in Table 4. A total of 16 points were plotted on the vertical face of the wall of the chamber. On each point, the respective value of the rebound number was noted (as shown in the table) and subsequently matched with the "A" line of the graph. An average compressive strength of 21 MPa (3,045 psi) has been reported at 28 days of age. A similar study was done by Sanchez and Tarranza [26], stating that there is a variation of a max of 10% from actual compressive strength when using a rebound hammer. However, in this study, the compressive strength is almost comparable to the target strength of the mix design, i.e., 3,000 psi.

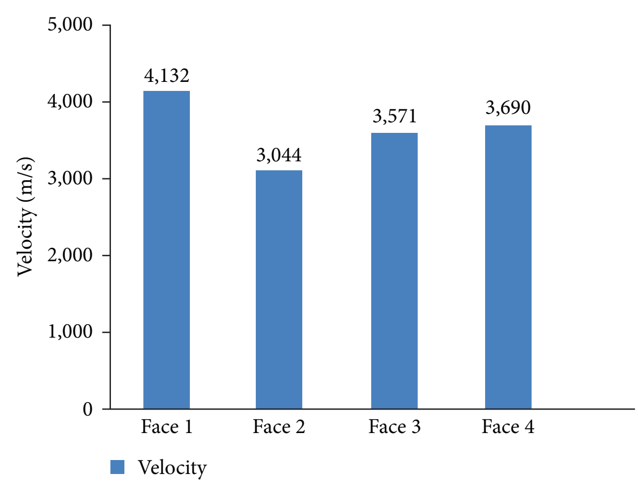

Figure 8: UPV data on each vertical face of the chamber.

3.1.3. PUNDIT. Ultrasonic pulse velocity values were noted for every face of the wall using the direct method of measurement, where the receiver and transmitter were in the same line of contact. The calculated values are summarized in Figure 8. It can be observed that there is no honeycombing in the concrete matrix as the majority values of pulse velocity lie between 3,500 and 4,500 m/s, which are typical values for

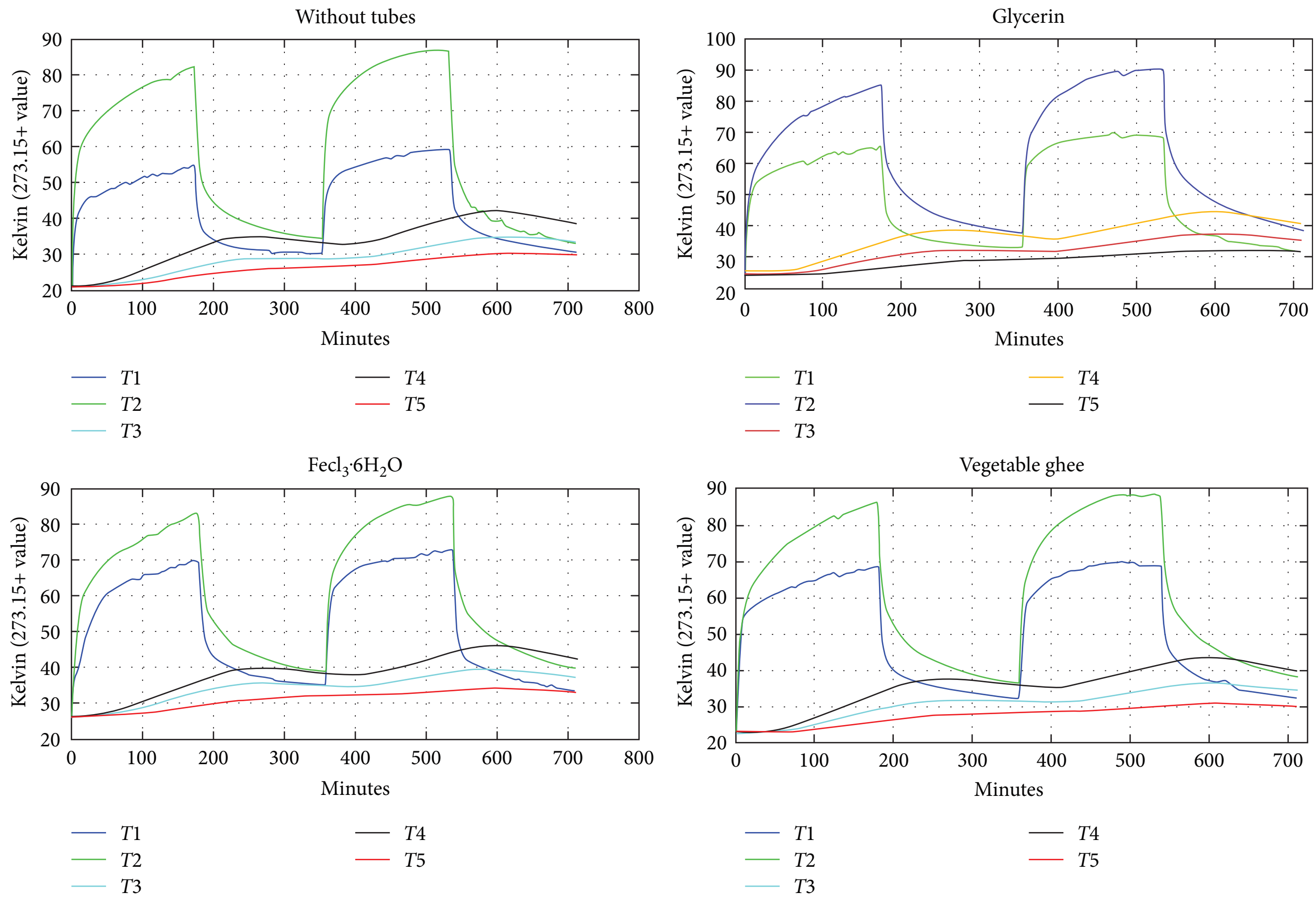

Figure 9: Variation of temperature record at sensors $T1$, $T2$, $T3$, $T4$, and $T5$ (3 hr testing cycle).

concrete having tight packing and no honeycombing effects. However, the same method was adopted by Chew [27] to assess the health of fire-damaged concrete.

3.2. Thermal Performace. Results for each testing cycle, i.e., 3 and 4 hr, are summarized as follows.

3.2.1. Three-Hour Testing Cycle. Figures 9 and 10 show the results for the 3-hr testing cycles of all four specimens at different temperature locations. It is observed that at sensor $T5$, the maximum temperature is achieved for the case with hollow tubes (without PCM), just like the study done by Kalbasi [28], in which five PCMs (PCM-20–PCM-24) were selected, and their behavior was studied. Vegetable ghee has performed best among all three PCM materials, as shown in Figure 10(a). At sensors $T3$ and $T4$, which were installed on the inner surface of the concrete wall, glycerin has given the best performance when used as PCM in hollow tubes of the concrete wall.

3.2.2. Two-Hour Testing Cycle. Figures 11and 12, as shown below, represent the result of the test specimen.

Based on the results cited above (Figure 11), the following is observed:

(a) Over the completion of tests, i.e., 12 hr, all the incorporated PCMs have shown positive results. The temperature decrease over the test completion time is almost 5 K. Ferric chloride, in this case, shows the best performance. Initially, the temperature rises, and after the melting point for ferric chloride is achieved, there is a tendency to reduce temperature, confirming the findings of other related studies [29, 30].

(b) On the other hand, it may be observed that vegetable ghee and glycerin performance was very effective in the first half of the test, i.e., to 400 min. The performance drops down with the increase in the temperature and becomes less effective at the time of completion when compared with ferric chloride.

(c) From Figure 12, it can be seen that vegetable ghee and glycerin have been performing very well from the beginning till the completion of the test. Both glycerin and vegetable ghee show almost analog performance. Ferric chloride, in this case, initially attracted more heat, but this becomes at par with the case with no PCM incorporated. Vegetable ghee may perform much better, showing much better tendencies to lose heat when the cooling phase starts, as suggested by Sharifi et al. [31] when incorporating PCMs in gypsum boards.

(d) A continuous low temperature is noted for vegetable ghee. Ferric chloride attracts more heat in the temperature range of almost 303 K. Ferric chloride shows

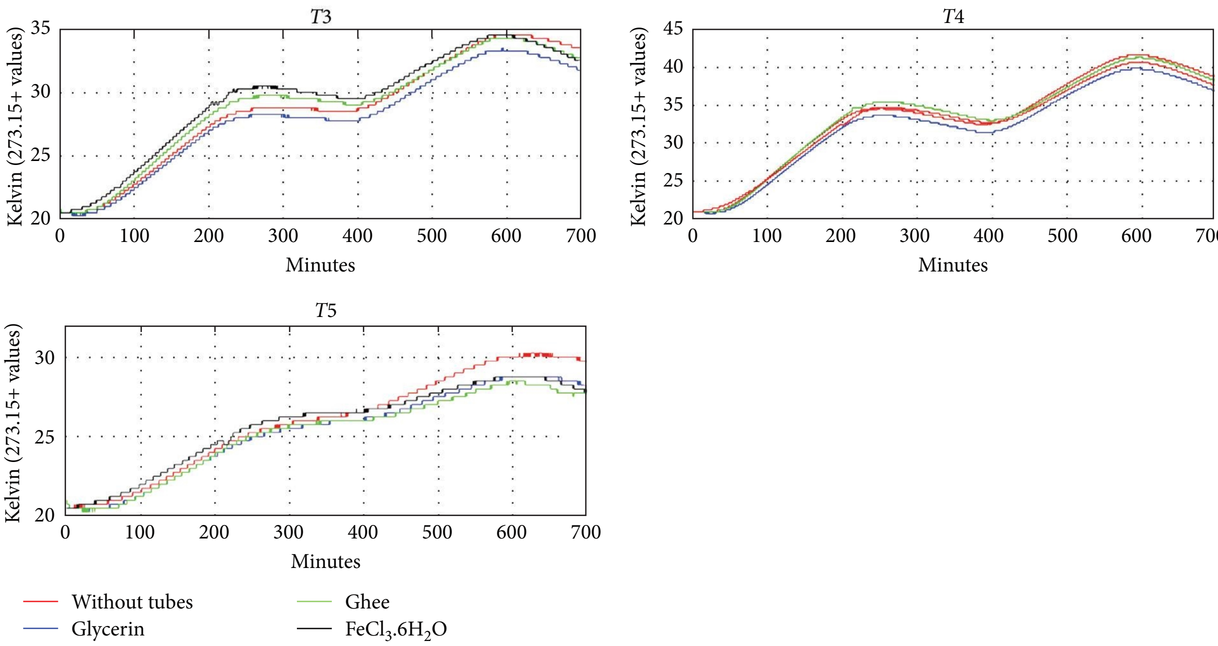

Figure 10: Variation of temperature at sensors $T3$, $T4$, and $T5$ for different conditions of the specimen (with and without PCM).

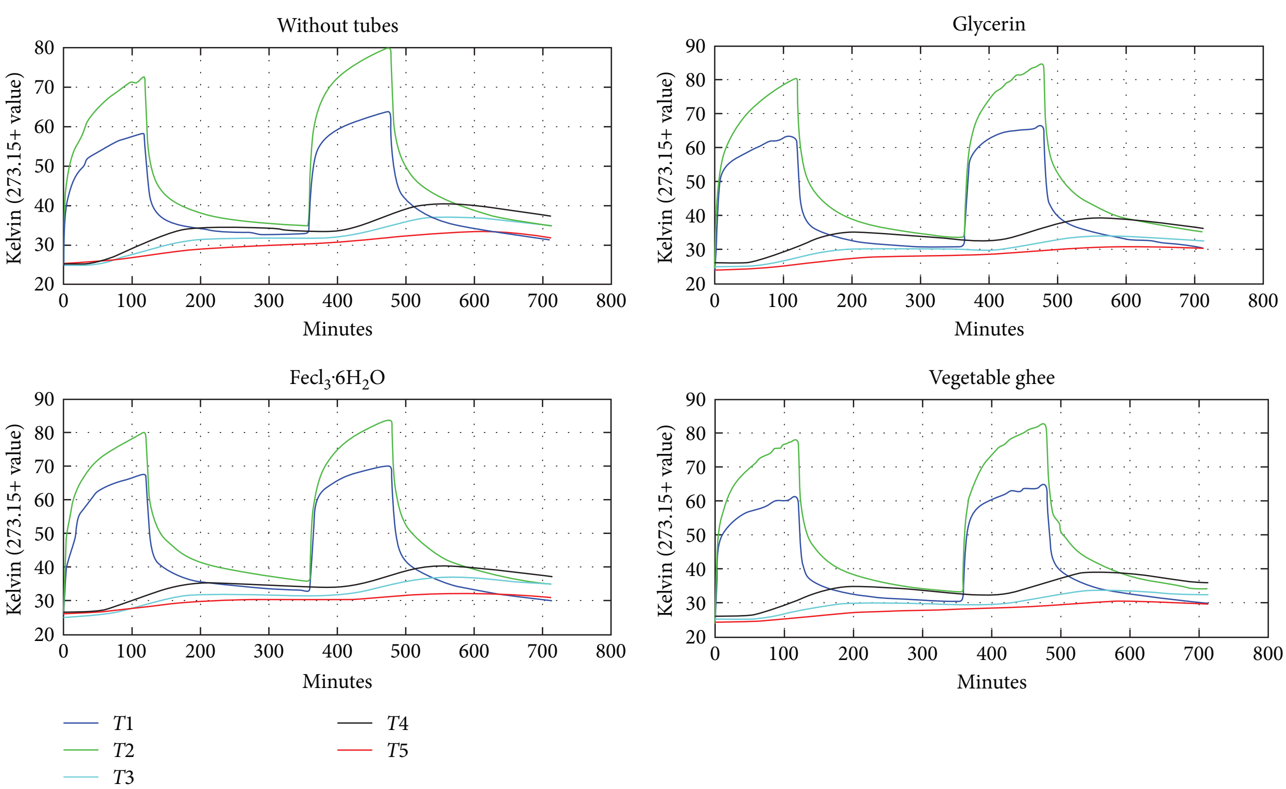

Figure 11: Temperature variation trends at various locations of sensors.

a much lower temperature on a further rise in temperature. Glycerin also shows a lower temperature for the heating in the first phase, but its tendency to lose heat is lower than vegetable ghee. Vegetable ghee and glycerin tend to attract less heat throughout the testing phase. Ferric chloride also shows a slow temperature rise for the heating in the second phase. However, in the first phase, the rise in temperature is the same as in the case without PCM, confirming the study done by Qu et al. [32].

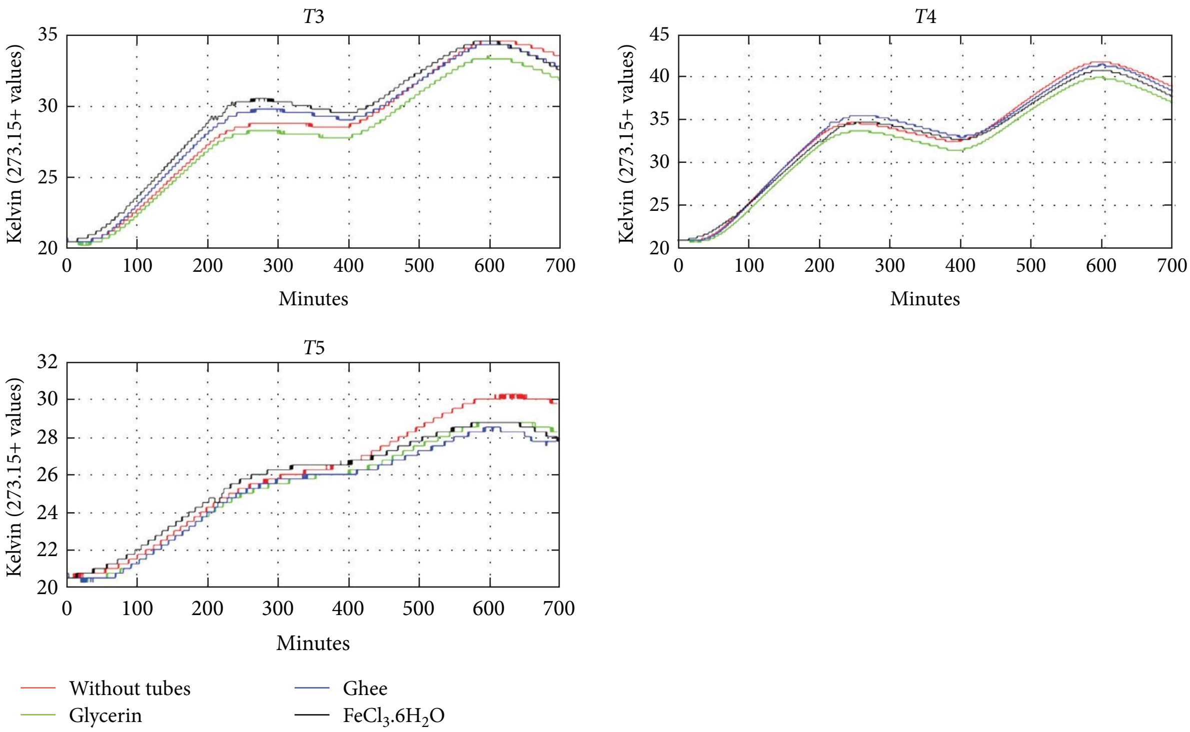

Figure 12: Temperature variation at sensors $T5$, $T4$, and $T3$.

4. Conclusions

All the PCMs are designed to maintain a temperature that is cozy and workable for the inhabitants. In this experimental work, an attempt has been made to explore locally available PCMs that are readily available and economical. The developed model was tested for temperature variations at five points. Out of these five points, three, namely $T3$, $T4$, and $T5$, were of utmost importance since they measured inside temperatures. The graphs plotted for the temperature for these three points have been discussed in the previous section.

The following conclusions have been drawn from the obtained results:

(a) Two PCMs, namely ferric chloride hexahydrate and vegetable ghee, performed well, and when compared to the case with no PCM, a temperature drop on the inner side was observed. However, glycerin worked as a sensible heat storage material and showed reduced temperature.

(b) It is concluded from the nondestructive testing that the variation in temperature is occurring due to the presence of PCM alone, as no honeycombing and strength deterioration was observed in the concrete mix.

(c) Among these available PCMs, the best performance was given by vegetable ghee, which showed a temperature drop for all the points, i.e., $T3$, $T4$, and $T5$.

(d) Vegetable ghee has a melting point of almost 308.15 K, the bearable prevalent temperature in the local environment. Over the completion of the test, i.e., 12 hr, all the incorporated PCM showed positive results and a maximum temperature loss of 2.25 K was reported.

(e) All the tests were carried out using the same model and embedded tubes. It has been observed that none of the PCM had any adverse effect.

(f) An increase in the cooling temperature results in better PCM performance, which may result in better energy efficiency.

(g) The heat load for the 1,000 1,000-W lamp at $T1$ and $T2$ sensors was observed to go as high as 361.15 K, which can be related to high temperatures during the daytime during summer, where temperature may reach upto 328.15 K in arid areas. For the purpose of studying temperature variation inside and outside the wall, a lamp of 1,000 W has been used as a source.

Data Availability

All the data used in the study are available within the manuscript.

Conflicts of Interest

The authors declare that there are no conflicts of interest of any kind.

References

[1] H. Cui, S. A. Memon, and R. Liu, “Development, mechanical properties and numerical simulation of macro encapsulated thermal energy storage concrete,” *Energy and Buildings*, vol. 96, pp. 162–174, 2015.

[2] A. Hanif, S. Diao, Z. Lu, T. Fan, and Z. Li, “Green lightweight cementitious composite incorporating aerogels and fly ash cenospheres—mechanical and thermal insulating properties,” *Construction and Building Materials*, vol. 116, pp. 422–430, 2016.

[3] S. A. Memon, H. Z. Cui, H. Zhang, and F. Xing, “Utilization of macro encapsulated phase change materials for the development of thermal energy storage and structural lightweight aggregate concrete,” *Applied Energy*, vol. 139, pp. 43–55, 2015.

[4] S. E. Kalnæs and B. P. Jelle, “Phase change materials and products for building applications: a state-of-the-art review and future research opportunities,” *Energy and Buildings*, vol. 94, pp. 150–176, 2015.

[5] A. R. Sakulich and D. P. Bentz, “Incorporation of phase change materials in cementitious systems via fine lightweight aggregate,” *Construction and Building Materials*, vol. 35, pp. 483–490, 2012.

[6] S. A. Memon, “Phase change materials integrated in building walls: a state of the art review,” *Renewable and Sustainable Energy Reviews*, vol. 31, pp. 870–906, 2014.

[7] H. Akeiber, P. Nejat, M. Z. A. Majid et al., “A review on phase change material (PCM) for sustainable passive cooling in building envelopes,” *Renewable and Sustainable Energy Reviews*, vol. 60, pp. 1470–1497, 2016.

[8] L. Zalewski, A. Joulin, S. Lassue, Y. Dutil, and D. Rousse, “Experimental study of small-scale solar wall integrating phase change material,” *Solar Energy*, vol. 86, no. 1, pp. 208–219, 2012.

[9] A. Sharma, V. V. Tyagi, C. R. Chen, and D. Buddhi, “Review on thermal energy storage with phase change materials and applications,” *Renewable and Sustainable Energy Reviews*, vol. 13, no. 2, pp. 318–345, 2009.

[10] M. Kalousck and J. Hirs, “Simulation of the summer indoor thermal comfort by using wallboard with phase change material,” Eurosun, Bologna, 2002.

[11] X. Shi, S. A. Memon, W. Tang, H. Cui, and F. Xing, “Experimental assessment of position of macro encapsulated phase change material in concrete walls on indoor temperatures and humidity levels,” *Energy and Buildings*, vol. 71, pp. 80–87, 2014.

[12] B. Xu and Z. Li, “Performance of novel thermal energy storage engineered cementitious composites incorporating a paraffin/diatomite composite phase change material,” *Applied Energy*, vol. 121, pp. 114–122, 2014.

[13] C. V. Podara, I. A. Kartsonakis, and C. A. Charitidis, “Towards phase change materials for thermal energy storage: classification, improvements and applications in the building sector,” *Applied Sciences*, vol. 11, no. 4, Article ID 1490, 2021.

[14] N. H. Abu-Hamdeh and K. A. Alnefaie, “Assessment of thermal performance of PCM in latent heat storage system for different applications,” *Solar Energy*, vol. 177, pp. 317–323, 2019.

[15] M. Zare and K. S. Mikkonen, “Phase change materials for life science applications,” *Advanced Functional Materials*, vol. 33, no. 12, Article ID 2213455, 2023.

[16] S. Nagar and P. K. Singh, “A short review on the industrial applications of phase change materials,” *IOP Conference Series: Materials Science and Engineering*, vol. 1116, no. 1, Article ID 012006, 2021.

[17] M. M. Awad, O. K. Ahmed, O. M. Ali et al., “Photovoltaic thermal collectors integrated with phase change materials: a comprehensive analysis,” *Electronics*, vol. 11, no. 3, Article ID 337, 2022.

[18] G. Asefi, T. Ma, and R. Wang, “Parametric investigation of photovoltaic-thermal systems integrated with porous phase change material,” *Applied Thermal Engineering*, vol. 201, Article ID 117727, 2022.

[19] F. Orsini, P. Marrone, S. Santini et al., “Smart materials: cementitious mortars and PCM mechanical and thermal characterization,” *Materials*, vol. 14, no. 15, Article ID 4163, 2021.

[20] P. Kulkarni and A. Muthadhi, “Thermal energy storage cement mortar with direct incorporation of organic and inorganic phase change materials,” *Innovative Infrastructure Solutions*, vol. 6, no. 1, Article ID 30, 2021.

[21] F. Rebelo, A. Figueiredo, R. Vicente, and V. M. Ferreira, “Study of a thermally enhanced mortar incorporating phase change materials for overheating reduction in buildings,” *Journal of Energy Storage*, vol. 46, Article ID 103876, 2022.

[22] S. Cunha, P. Leite, and J. Aguiar, “Characterization of innovative mortars with direct incorporation of phase change materials,” *Journal of Energy Storage*, vol. 30, Article ID 101439, 2020.

[23] ASTM C143/C143M, “Standard test method for slump of hydraulic-cement concrete,” pp. 1–4, 2015, Astm C143.

[24] ASTM C805/C805M-18, *Standard test method for rebound number of hardened concrete*pp. 1–4, 2015.

[25] ASTM C597-22, “Ultrasonic pulse velocity through concrete,” pp. 1–4, 2022, 1, ASTM Int.

[26] K. Sanchez and N. Tarranza, “Reliability of rebound hammer test in concrete compressive strength estimation,” *International Journal of Advances in Agricultural & Environmental Engineering*, vol. 1, no. 2, 2015.

[27] M. Y. L. Chew, “The assessment of fire damaged concrete,” *Building and Environment*, vol. 28, no. 1, pp. 97–102, 1993.

[28] R. Kalbasi, “Usefulness of PCM in building applications focusing on envelope heat exchange—energy saving considering two scenarios,” *Sustainable Energy Technologies and Assessments*, vol. 50, Article ID 101848, 2022.

[29] S. A. Mohamed, F. A. Al-Sulaiman, N. I. Ibrahim et al., “A review on current status and challenges of inorganic phase change materials for thermal energy storage systems,” *Renewable and Sustainable Energy Reviews*, vol. 70, pp. 1072–1089, 2017.

[30] X. Huang, G. Alva, Y. Jia, and G. Fang, “Morphological characterization and applications of phase change materials in thermal energy storage: a review,” *Renewable and Sustainable Energy Reviews*, vol. 72, pp. 128–145, 2017.

[31] N. P. Sharifi, A. A. N. Shaikh, and A. R. Sakulich, “Application of phase change materials in gypsum boards to meet building energy conservation goals,” *Energy and Buildings*, vol. 138, pp. 455–467, 2017.

[32] Y. Qu, D. Zhou, F. Xue, and L. Cui, “Multi-factor analysis on thermal comfort and energy saving potential for PCM-integrated buildings in summer,” *Energy and Buildings*, vol. 241, Article ID 110966, 2021.